

# Kernel dependence of the Gaussian Process reconstruction of late Universe expansion history

Joseph P Johnson,<sup>a</sup> H. K. Jassal<sup>a,b</sup>

<sup>a</sup>Indian Institute of Science Education and Research, Mohali, knowledge city, Sector 81, Manauli, PO, Sahibzada Ajit Singh Nagar, Punjab 140306, India

<sup>b</sup>National Centre for Radio Astrophysics, Tata Institute of Fundamental Research, Pune-411 007, India.

E-mail: [josephj@iisermohali.ac.in](mailto:josephj@iisermohali.ac.in), [hkjassal@iisermohali.ac.in](mailto:hkjassal@iisermohali.ac.in)

**Abstract.** In this work, we discuss model-independent reconstruction of the expansion history of the late Universe. We use Gaussian Process Regression to reconstruct the evolution of various cosmological parameters such as  $H(z)$  and slow-roll parameter using observational data to train the GP model. We look at the GP reconstruction of these parameters using stationary and non-stationary kernel functions. We examine the effect of the choice of kernel functions on the reconstructions. We find that non-stationary kernels such as polynomial kernels might be a better choice for the reconstruction if the training data set is noisy (such as  $H(z)$  data) as it helps to avoid fitting the error in the data. We also look at the kernel dependence of other cosmological parameters such as the redshift of transition to the accelerated expansion. This has been achieved by reconstructing the derivatives of the expansion history ( $H(z)$ ) such as the deceleration parameter/slow-roll parameter.

---

<sup>1</sup>Corresponding author.

---

## Contents

<b>1</b>	<b>Introduction</b>	<b>1</b>
<b>2</b>	<b>Late Universe Cosmology</b>	<b>3</b>
<b>3</b>	<b>Gaussian Process and choice of kernels</b>	<b>4</b>
<b>4</b>	<b>Cosmological parameters and datasets</b>	<b>5</b>
<b>5</b>	<b>Results</b>	<b>6</b>
<b>6</b>	<b>Conclusions and discussion</b>	<b>9</b>
<b>A</b>	<b>Results for Matern-7/2 and Poly-2,3 kernels</b>	<b>10</b>

---

## 1 Introduction

Cosmological parameters continue to be determined to better and better precision. The availability of a large amount of good quality and diverse datasets is a key factor in getting to this precision. The datasets include observations of the type Ia supernovae, Baryon acoustic oscillations (BAO), Cosmic Microwave Background (CMB) Radiation, direct measurements of the Hubble parameter, and more recently, dark energy survey and dark energy spectroscopic instrument data [1–3]. These different datasets probe different cosmological quantities and their combinations give very tight constraints on the cosmological parameters. One of the most significant breakthroughs in cosmology happened when observations of Type Ia supernovae revealed that the expansion of the late Universe is accelerating [4]. This observation required the introduction of dark energy to the standard cosmological model, as ordinary matter or dark matter could not explain the accelerated expansion. The nature of dark energy is not known, although the cosmological constant is a simple and an elegant explanation. The  $\Lambda$ CDM model, a cosmological constant and cold dark matter universe model has been highly successful in explaining various cosmological observations [4–6]. However, the known theoretical problems such as fine-tuning problem and coincidence problem indicated that one might have to look at the alternatives to the  $\Lambda$ CDM model [7–9].

Typically, the alternatives include those based on the assumption that dark energy is a fluid, and those where the model is described by a scalar field and various other descriptions [10]. There have been many dynamic dark energy models proposed including parametric models such as CPL model, scalar field models like quintessence and k-essence, all within the framework of GR [9, 11–18]. Modified gravity theories such as  $f(R)$  gravity models also have been considered to be viable alternatives [19–23]. However, none of these models have been able to solve the issues completely [24, 25]. With these issues, it is important to obtain the expansion history of the Universe from the observations in a model-independent manner [26, 27]. There have been methods of model-independent reconstruction of the Hubble parameter. One of the most popular methods is cosmography, where the Hubble parameter is expanded as a Taylor series expansion using its derivatives [28–31]. Although it gives the evolution of the Hubble parameter without assuming any underlying model, at higher redshifts, it falls short

of the desired accuracy. Hence we need to look for a better reconstruction method that is model-independent and accurate in the redshift range of observations [32–37].

Moreover, as the observations became more accurate and precise, discrepancies between the cosmological parameters estimated from the late and early Universe observations using  $\Lambda$ CDM model were revealed, most prominent of them being the  $H_0$  tension and the  $\sigma_8$  tension [24, 25, 38]. Therefore there is still room for improvement in determining cosmological parameters; this is especially true in constraining dark energy equation of state parameter. While there are theoretical models that attempt to solve this problem, attempts are also underway to understand if calibration and systematics are the main reasons for this tension [39, 40]. Since there is no reason to prefer one phenomenological model over the other, model-independent methods of cosmological parameter fitting are therefore needed to reconstruct the expansion history of the Universe. A theoretical reconstruction can be done by determining the form of a scalar field potential or a fluid parameterisation by assuming an evolution history of the scale factor [41–44].

The expansion history of the Universe can be reconstructed with methods that do not assume an underlying cosmological model. Such methods include the Principal Component Analysis, Singular Value Decomposition, Gaussian Processes, Artificial Neural Networks and other machine learning tools [45–53]. While being efficient tools in cosmology; all the methods have their own individual merits and limitations. For example, the principal component analysis is very sensitive to the errors in the data and is also sensitive to outliers which makes the analysis unreliable. Moreover, the nonlinear relations between cosmological quantities can lead to spurious results [26, 54]. Similarly, single value decomposition also assumed linearity [55]. Gaussian Processes are also a powerful tool which is now in use for cosmological analysis [30, 56–58].

By definition, any subset of a Gaussian Process follows a multivariate Gaussian distribution. This property can be used to predict the mean and variance of a new test point using a closed-form equation [59]. This makes it a powerful regression tool to reconstruct the expansion history of the Universe using the available data points. Compared to other regression/interpolation tools, the Gaussian Process has the advantage of being model-independent and being able to predict the Gaussian error at a test point in addition to the mean value, making it an ideal tool to study the derived cosmological parameters as well [30, 56, 58, 60]. There are some challenges using the Gaussian Process Regression in cosmological studies. Gaussian Process regression can be computationally expensive when dealing with larger data sets. However, it is not a concern for this analysis. One also has to be careful with the choice of the kernel functions as it can significantly affect the reconstruction of the expansion history as well as the derived cosmological parameters.

In this paper, we explore the reconstruction of the cosmological expansion history using Gaussian Process Regression. The motivation of this work is to understand how the choice of a kernel affects the allowed range and evolution of the parameters. For this purpose, we use the stationary kernels and a non-stationary kernel. We show that the choice of stationary kernels such as Radial Basis Function (RBF) and Matern kernels is consistent with a second phase of accelerated expansion at higher redshifts in addition to the one that Universe is undergoing currently. Polynomial kernels result in a reconstruction of the evolution that is similar to the one predicted by the  $\Lambda$ CDM model. However, as the degree of the polynomial kernel increases, the reconstructions tend to become similar to the ones corresponding to the RBF and Matern kernels.

The paper is organised in the following manner. Section 2 reviews the late universe cos-

mology. The following section 3 introduces Gaussian Processes and different kernels followed by a discussion on the datasets used in this work in Section 4. The results of the work are presented in Section 5 and the concluding Section 6 summarises the main results.

## 2 Late Universe Cosmology

The universe being isotropic and homogeneous at large enough scales constitutes the central idea of the cosmological principle, which is mathematically represented by the Friedmann-Lemaitre-Robertson-Walker (FLRW) metric (for a spatially flat Universe) given by

$$ds^2 = -dt^2 + a(t)^2 (dx^2 + dy^2 + dz^2), \quad (2.1)$$

where the time evolution of the Universe is encoded in the scale factor  $a(t)$ . The Universe is found to be expanding from the observation of the redshift of the distant galaxies. Expansion of the universe can be quantified by the Hubble parameter defined by

$$H(t) = \frac{\dot{a}}{a}. \quad (2.2)$$

In an expanding Universe ( $H(t) > 0$ ), farther galaxies would appear to be receding at a larger speed to the observer, increasing the redshift of the light source. Since an observer would be looking into the past while observing farther sources, the redshift  $z$  can be used as a convenient replacement for the time coordinate  $t$ . Both of these variables are related to each other via the following relations.

$$a = \frac{1}{1+z}, \quad \frac{df}{dt} = -(1+z)H(z)\frac{df}{dz} \quad (2.3)$$

where  $f$  is any dynamic variable of interest. Since redshift is directly observable, most of the cosmological observations use redshift as the stand-in for the time coordinate. The expansion of the Universe can be accelerating or decelerating depending on the dominant matter/energy component at the epoch. The acceleration of the universe can be quantified by the slow-roll parameter

$$\epsilon(z) = -\frac{\dot{H}}{H^2} = (1+z)\frac{H'}{H} = q + 1 \begin{cases} \epsilon < 1 : \text{accelerating} \\ \epsilon \geq 1 : \text{decelerating} \end{cases} \quad (2.4)$$

where  $q$  is the deceleration parameter. For an accelerating Universe,  $\epsilon < 1$  ( $q < 0$ ). The kinematics parameters can be extended to higher derivatives of the scale factor, namely jerk and snap parameters corresponding to the third and fourth derivatives of the scale factor respectively. The efficacy of this method is however limited to lower redshifts. In this analysis, we focus on the deceleration parameter assuming that the contribution of the other statefinder parameters is very small and the reconstruction is not sensitive to them.

Cosmological observations provide us with the information regarding the evolution of various cosmological parameters. Although the volume and accuracy of the observational data have increased, the data points are at discrete redshifts and there can be large gaps in these datasets. To study the time evolution of the cosmological parameters, it is important to construct the continuous time evolution of the cosmological parameters from the discrete data points from the observations. Various regression methods have been used for this purpose. In this work, we use the Gaussian Process Regression, which is discussed in detail in the next section.

### 3 Gaussian Process and choice of kernels

Among the various methods of reconstruction of the expansion history of the Universe, Gaussian Process Regression stands out due to its ability to predict the mean value as well as the variance of the observable at any given test point. Since the derivative of the Gaussian Process is also a Gaussian Process, it has the added benefit of predicting the evolution of the derived cosmological parameters such as the slow-roll parameter using the observational data.

A Gaussian Process is a collection of random variables, any finite number of which have a joint Gaussian distribution [61]. Assume that we have a data set  $y(x)$  with mean  $m(x)$ , and covariance matrix given by  $k_y(x, x)$ , and  $f$  represents the reconstructed function value that is not present in the data. Then in the Gaussian Process, the joint probability distribution of the data  $y$  and unknown test data point  $f$  is given by [30]

$$\begin{bmatrix} \mathbf{y} \\ \mathbf{f} \end{bmatrix} \sim \mathcal{N} \left( \begin{bmatrix} \mathbf{m}(\mathbf{x}) \\ \mathbf{m}(\mathbf{x}_*) \end{bmatrix}, \begin{bmatrix} k_y(x, x) & k(x, x_*) \\ k(x_*, x) & k(x_*, x_*) \end{bmatrix} \right) \quad (3.1)$$

The conditional distribution of  $\mathbf{f}$  given the data is described by

$$\bar{\mathbf{f}} = m(x_*) + k(x_*, x) k_y^{-1}(x, x) \mathbf{y} \quad (3.2)$$

$$\text{Cov}(\mathbf{f}) = k(x_*, x_*) - k(x_*, x) k_y^{-1}(x, x) k(x, x_*) \quad (3.3)$$

A Gaussian Process is completely specified by the mean and the covariance function. The covariance function is given by the sum of the kernel function and the covariance of the observed data. The hyperparameters in the mean function and the kernel function are optimized using the training dataset. Usually, the final reconstruction is independent of the prior mean function, and we use a zero mean function in this work. Gaussian Process regression has been used as an effective tool to reconstruct the expansion history, as it is completely model-independent, and the only user input in the reconstruction is the choice of the kernel/covariance function used. In this work, we use the Gaussian Process regression to reconstruct the evolution of the Hubble parameter and the slow-roll parameter using the  $H(z)$  observations as the training data set.

We consider kernels that are stationary (RBF, Matern) and non-stationary (Polynomial-d).

- RBF kernel

$$k(x, \tilde{x}) = \sigma_f^2 \exp \left( -\frac{(x - \tilde{x})^2}{2\ell^2} \right) \quad (3.4)$$

- Matern- $\nu$

$$k(x, \tilde{x}) = \sigma_f^2 \frac{2^{1-\nu}}{\Gamma(\nu)} \left( \frac{\sqrt{2\nu} |x - \tilde{x}|}{\ell} \right)^\nu k_\nu \left( \frac{\sqrt{2\nu} |x - \tilde{x}|}{\ell} \right) \quad (3.5)$$

where  $\Gamma$  is the Gamma function, and  $k_\nu$  is the Bessel function of the second kind.

- Polynomial kernel

$$k(x, \tilde{x}) = \sigma_f^2 (x\tilde{x} + \ell)^d \quad (3.6)$$

In this work, we consider the cases  $d = 2, 3, 4, 6, 8$ .

Most of the widely used kernel functions such as Radial Basis Function (RBF) kernels and Matern kernels are stationary kernels, where the covariance depends only on the relative separation between the data points. The RBF kernel is a popular choice for the Gaussian Process regression over other kernel methods since it can adapt to the training data very well, and is infinitely differentiable, which will be useful while computing the derivatives of the relevant variables. It can also be thought of as an infinite sum of polynomial kernels or as a special case of Matern kernel where  $\nu \rightarrow \infty$ . However, in some situations, the flexibility of the RBF kernel can be a disadvantage as it can be "too smooth". As it is very flexible and results in smooth reconstructions, the RBF kernel can also fit the error inaccuracies in the data, which can be difficult to detect and hence needs a careful interpretation. The risk of over-fitting is significant if the error or inaccuracies in the training data are high, as is the case of  $H(z)$  data, especially the data points obtained from the cosmic chronometer observations.

The use of polynomial kernels can be motivated by the linear regression method. It can be shown that the kernel function is related to the basis functions used for the linear regression [62]. If a function can be expanded in terms of polynomials, the corresponding Gaussian Process regression can be obtained using the polynomial kernels. It has been shown that the late Universe expansion history can be expressed as a finite polynomial expansion with the cosmography method [28]. This indicates that we can use the Polynomial kernel for the Gaussian Process reconstruction of the late-Universe expansion history. There is also less chance of the model overfitting or fitting the error in the data. However, with polynomial kernels, there is a risk of the covariance values diverging at high redshift values leading to instabilities. For the datasets considered here, it has been verified that no such instabilities occur. The reduced flexibility of the polynomial kernels can be overcome by considering the higher-order kernel. In this work, we focus on the Poly-4,6,8 kernels. The results for the Poly-2,3 kernels are presented in Appendix A.

## 4 Cosmological parameters and datasets

We use the following four different compilations of  $H(z)$  data to reconstruct the late Universe expansion history.

1. **H<sub>z</sub> 57** : Hubble parameter data compiled in Ref. [63], contains data points from Cosmic Chronometer (**CC 32**) and BAO (**BAO 18**) observations. Covers the redshift range  $0.07 \leq z \leq 2.36$ .
2. **CC 32** : Hubble parameter data from the Cosmic Chronometer observations compiled in Ref. [64]. Covers the redshift range  $0.07 \leq z \leq 1.965$ .
3. **BAO 18** : Hubble parameter data from the BAO observations compiled in Ref. [64]. Covers the redshift range  $0.24 \leq z \leq 2.36$ .
4. **BAO 15**: Hubble parameter data from the BAO observations compiled in Ref. [64], excluding the three highest redshift values from BAO 18 mentioned above. This covers the redshift range  $0.24 \leq z \leq 0.64$ . We do a separate analysis to check if the large gap between the high and low redshift data points has any effect on the analysis.

These datasets describe the value of the Hubble parameter at given redshifts, along with the uncertainty. We use the data sets to train the Gaussian Process model to predict the value of the Hubble parameter along with the uncertainty at the unobserved redshifts. We

use the GaPP package<sup>12</sup> [56] modified to implement the polynomial kernels to reconstruct the Hubble parameter and its derivatives.

We analyse the evolution of the Hubble parameter reconstructed by the Gaussian Process using (i) RBF kernel, (ii) Matern-7/2 kernel, (iii) Polynomial-d kernel,  $d = \{2, 3, 4, 6, 8\}$ . We also reconstruct the derivative of the Hubble parameter along with its uncertainty using the GaPP package. It is then used to study the slow-roll parameter  $\epsilon$ . Uncertainty in the evolution of  $\epsilon$  is obtained using the method of propagation of errors. The value of  $\epsilon$  tells us if the expansion is accelerated or decelerated and gives the redshift of transition between accelerated and decelerated phases. It has to be noted that we are not comparing the results obtained for each data set. The effect of combining the datasets and the effect of individual datasets on the analysis will be the topic of a follow-up analysis.

## 5 Results

Reconstruction of the Hubble parameter along with the uncertainty corresponding to the different kernels and datasets are given in Fig. 1. From the plots, we see that the reconstructions fit the datasets well. This is verified by comparing the  $\chi^2$  values (Table 1) corresponding to each of the kernels, and we see that they all give a good fit for the data. We have also included the  $\chi^2$  values for the best fit  $\Lambda$ CDM model obtained using MCMC analysis for each of the datasets for comparison. We see that, for a given dataset, the  $\chi^2$  values corresponding to the GP reconstructions and the best fit  $\Lambda$ CDM model are comparable. This indicates that the GP reconstruction results in a good fit for the data as compared to the model-dependent reconstructions using the MCMC analysis of the data. Since the results for the RBF kernel and Matern kernels are nearly identical, the results obtained using the latter are given in the appendix. Results for the Poly2 and Poly3 kernels are also presented in the appendix. From the parameter constraints for the  $\Lambda$ CDM model, we see that parameter values are closer to the Planck-2018 values for the **CC 32** and **BAO 15** data sets. This will be further explored in a future work.

	RBF	Poly4	Poly6	Poly8	Best fit $\Lambda$ CDM		
	$\chi^2$	$\chi^2$	$\chi^2$	$\chi^2$	$\chi^2$	$H_0$	$\Omega_\Lambda$
Hz 57	41.785	42.729	42.743	42.378	44.150	$69.987_{-1.100}^{1.082}$	$0.735_{-0.018}^{0.016}$
CC 32	14.250	14.945	14.952	14.613	14.549	$67.762_{-3.114}^{3.042}$	$0.673_{-0.065}^{0.055}$
BAO 18	8.995	9.189	9.203	9.112	11.693	$71.071_{-1.331}^{1.305}$	$0.746_{-0.019}^{0.018}$
BAO 15	9.594	8.491	8.450	8.426	8.600	$66.179_{-3.092}^{2.984}$	$0.637_{-0.078}^{0.066}$

**Table 1.** The table shows  $\chi^2$  values of the reconstructions and the best fit  $\Lambda$ CDM models. The results are comparable for each individual dataset.

By looking at the reconstruction of the evolution of the Hubble parameter, we see that there are some differences in the reconstruction using the stationary and non-stationary kernels, especially at higher redshifts. To understand it better, we look at the slow-roll parameter ( $\epsilon$ ), which tells us whether the Universe is accelerating or decelerating, and the redshift of transition ( $z_t$ ) from a decelerated to the accelerated Universe.

<sup>1</sup>GaPP repository

<sup>2</sup>GaPP for Python3

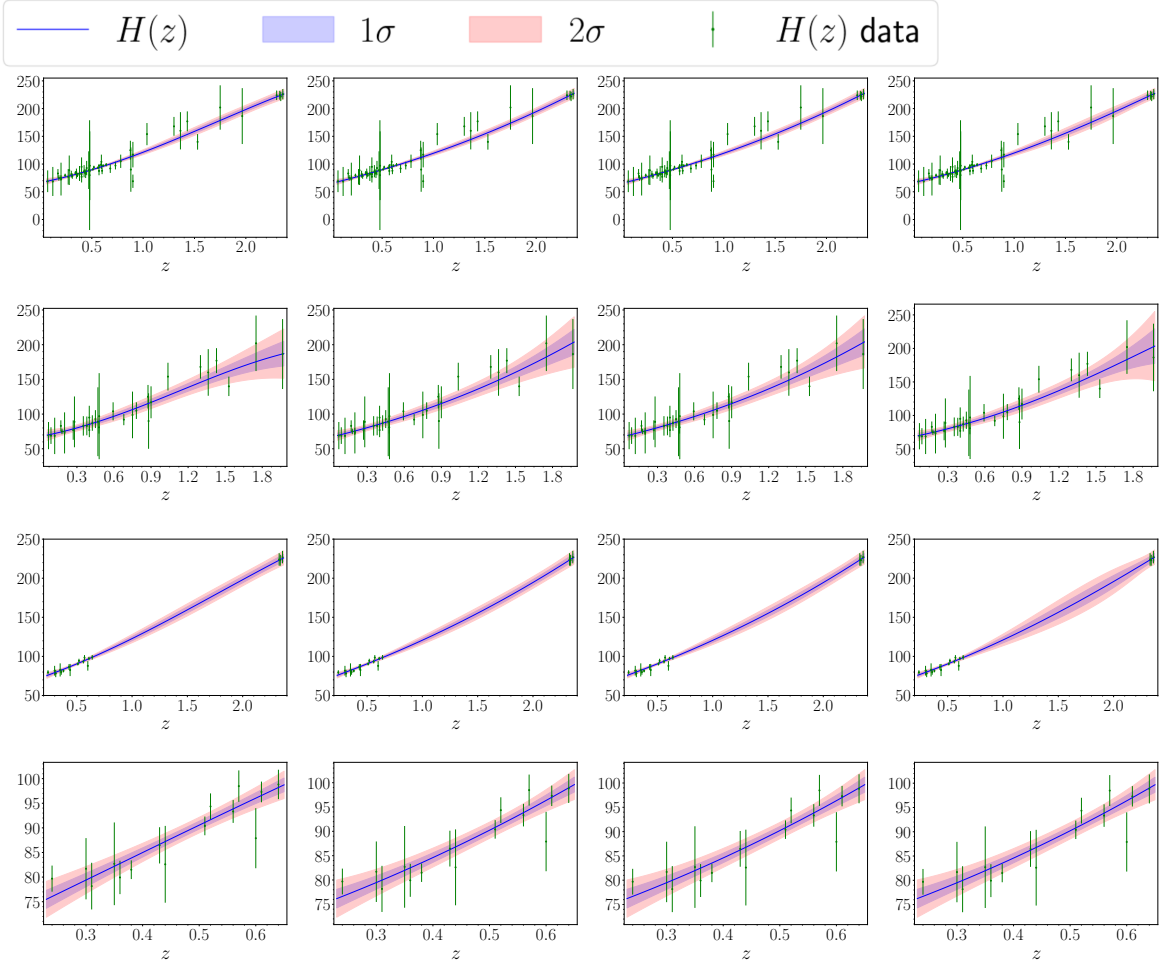


**Figure 1.** This figure shows the reconstructed evolution of the Hubble parameter. Top to bottom: Hz 57, CC 32, BAO18, BAO15. Left to right: RBF, Poly4, Poly6, Poly8

Transition redshifts for different kernels and the best fit  $\Lambda$ CDM are given in Fig. 1 and Table 5. We see that all the reconstructions are consistent with the current accelerated expansion of the Universe. In the case of the polynomial kernels and the best-fit  $\Lambda$ CDM models, within the considered redshift range, the Universe undergoes a transition from decelerated to accelerated expansion. The value of  $z_t$  is different for the different data sets, especially so for the BAO 15 data, which covers only the lower redshifts. Polynomial kernels result in similar values of  $z_t$ . However, for RBF and Matern kernels with the CC 32 dataset, the current accelerated phase is preceded by a decelerated phase and another accelerated phase before that, resulting in two different transition redshifts within the given redshift range. One can also see a similar trend in the case of Hz 57 and BAO 18 datasets, where it seems that there is an accelerated phase just above the given redshift range of the data. For the low-redshift BAO data (BAO 15), the transition does not happen within the given redshift range, and the Universe is always accelerating in the given redshift range.

We also see that the transition redshifts for the best-fit  $\Lambda$ CDM models are closer to the one corresponding to the polynomial kernel reconstructions as compared to the stationary kernel reconstructions. Excluding the low-redshift BAO 15 dataset, the  $z_t$  values for the GP

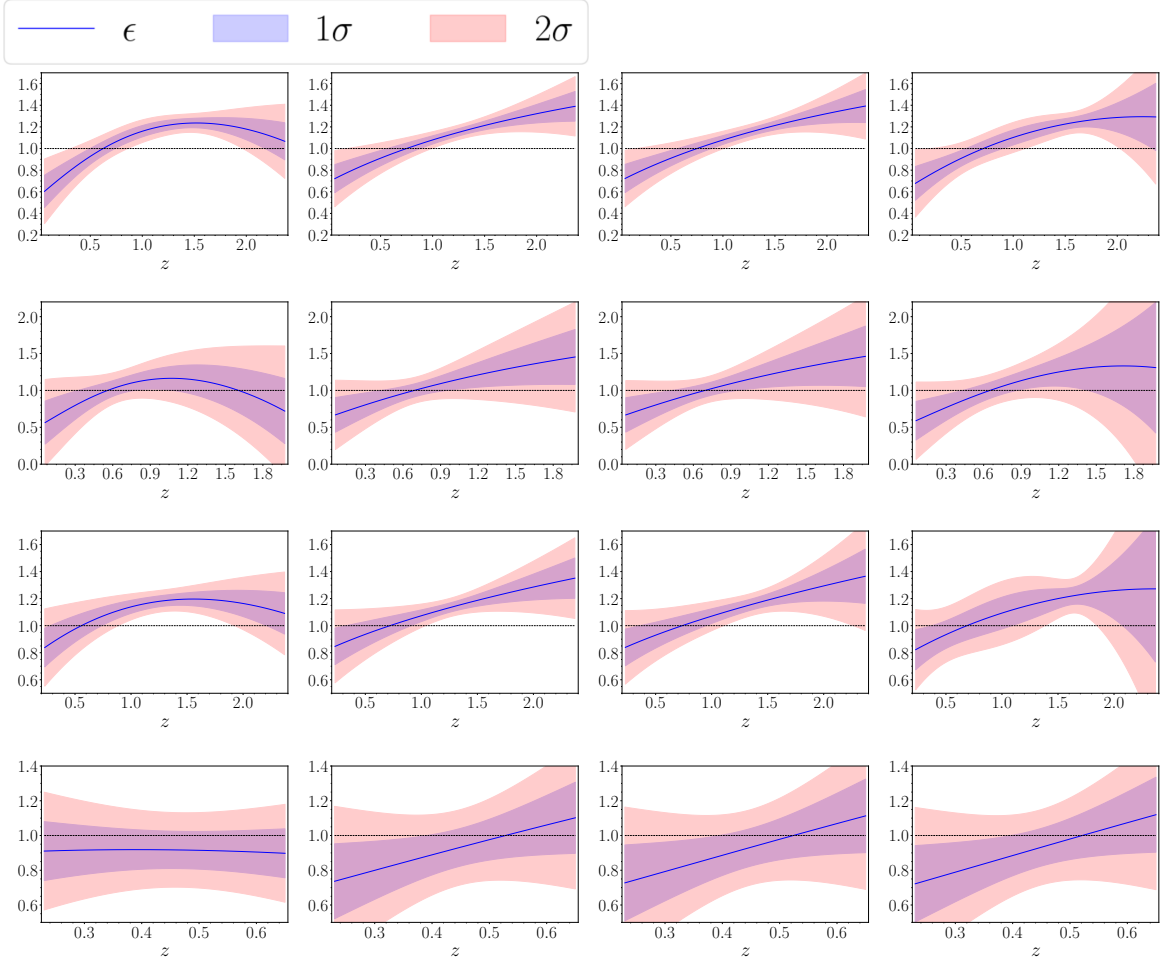


**Figure 2.** This figure shows the evolution of the slow-roll parameter  $\epsilon$ . Top to bottom: Hz 57, CC 32, BAO18, BAO15. Left to right: RBF, Poly4, Poly6, Poly8. There are multiple accelerated phases in the reconstructions using the RBF kernel.

reconstruction with a given kernel have similar values across the datasets, which is not the case for the best fit  $\Lambda$ CDM models. Interestingly, as the degree of the polynomial increases, the behaviour of the evolution becomes more similar to that of the RBF kernel. It is consistent with the fact that the RBF kernel can be considered as an infinite sum of polynomial kernels.

	RBF		Poly4		Poly6		Poly8		$\Lambda$ CDM	
	$z_{t_1}$	$z_{t_2}$	$z_{t_1}$	$z_{t_2}$	$z_{t_1}$	$z_{t_2}$	$z_{t_1}$	$z_{t_2}$	$z_{t_1}$	$z_{t_2}$
Hz 57	0.6242	-	0.7490	-	0.7513	-	0.7120	-	0.7732	-
CC 32	0.5603	1.6050	0.6906	-	0.6925	-	0.6504	-	0.6222	-
BAO 18	0.5577	-	0.7205	-	0.7376	-	0.6862	-	0.8106	-
BAO 15	-	-	0.5280	-	0.5238	-	0.5213	-	0.5396	-

**Table 2.** Transition redshifts for the reconstructions and best fit  $\Lambda$ CDM models. There are multiple accelerated phases in the reconstruction using the **CC 32** and the RBF kernel.

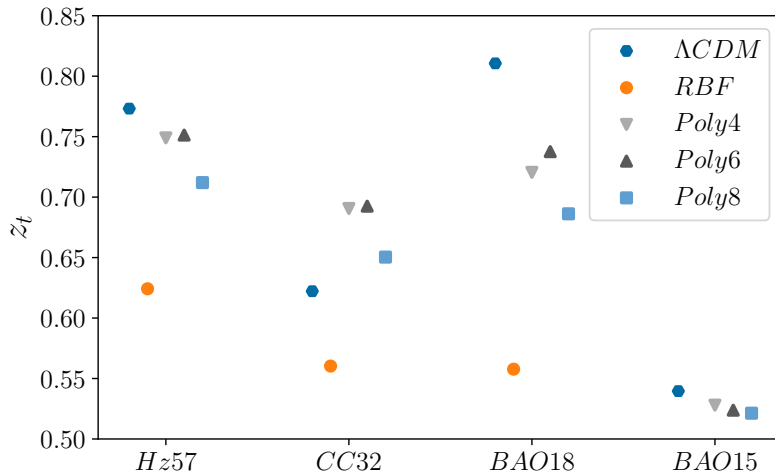


**Figure 3.** Late universe transition redshift  $z_t$  values for the GP reconstructions and the best-fit  $\Lambda$ CDM model for the different data-sets. The values corresponding to the Polynomial reconstructions lie closer to the  $\Lambda$ CDM values.

## 6 Conclusions and discussion

We have reconstructed the evolution of the Hubble parameter and slow-roll parameter using the Gaussian Process (GP) regression from the  $H(z)$  observational data while accounting for the uncertainties. These data sets include cosmic chronometer observations and  $H(z)$  estimated from the BAO observations. Two of the data sets (**BAO 18**, **BAO 15**) consist of data from the BAO observations, one contains the chronometer observations (**CC 32**), and the fourth one (**Hz 57**) contains the combination of both. For the GP reconstruction, we have used two stationary (RBF, Matern-7/2), and five non-stationary (Polynomial-2,3,4,6,8) kernels. As is evident from the  $\chi^2$  values, the GP reconstruction fits the data well and is comparable to the best-fit  $\Lambda$ CDM model. A visual inspection shows that the evolution of the Hubble parameter flattens out at higher redshifts in RBF reconstructions when compared to Polynomial reconstructions. The effect of the choice of kernel becomes more apparent in the reconstruction of the evolution of the slow-roll parameter. Reconstructions using the stationary kernels either show a second accelerated phase or a tendency to move towards one at higher redshifts, which is consistent with previous results in the literature [65]. This is more pronounced for the **CC 32** dataset, where the uncertainties in the data are larger. We also see the results for the higher-degree polynomials moving towards the ones corresponding to the RBF kernel.

Multiple accelerated phases could indicate new physics at the high redshift values within the dataset. But this is unlikely since it would mean a drastic departure from the evolution predicted by the current cosmological models that are consistent with observations. The other, more plausible explanation is that the RBF and Matern kernels are overfitting/fitting the errors, in the high redshift  $H(z)$  data points. The fact that the departure from the expected evolution is more drastic when there are large uncertainties in the observational data (**CC 32**) points in this direction. This problem can be fixed by using polynomial kernels, which even though more restrictive, capture the relevant information within the data. Polynomial kernels are also better when we need to extrapolate the evolution beyond the redshift range

available in the data. The availability of more accurate high redshift ( $z > 2$ ) data will help us to determine if the existence of two accelerated phases in the case of the stationary kernels is due to the choice of kernels or if it indicates any new physics.

In this work, we have looked at different  $H(z)$  datasets and showed the clear difference in the evolution of the cosmological parameters while using the stationary kernel such as RBF and Matern kernel, and non-stationary polynomial kernels. To confirm these findings, one needs to look at other datasets and study the evolution of the reconstructed cosmological parameters. This analysis can be made more rigorous by accounting for the covariances in the observational data while performing the GP reconstruction which will be subject of a future work.

## A Results for Matern-7/2 and Poly-2,3 kernels

Here we present the results for the Matern-7/2 and Poly-2,3 kernels. We see that the results for Matern and RBF kernels are nearly identical.

	RBF	Mat72	Poly2	Poly3	Best fit $\Lambda$ CDM		
	$\chi^2$	$\chi^2$	$\chi^2$	$\chi^2$	$\chi^2$	$H_0$	$\Omega_\Lambda$
Hz 57	41.7850	41.7794	42.6515	42.7107	44.150	$69.987^{1.082}_{-1.100}$	$0.735^{0.016}_{-0.018}$
CC 32	14.2502	13.5816	14.9008	14.9331	14.549	$67.762^{3.042}_{-3.114}$	$0.673^{0.055}_{-0.065}$
BAO 18	8.9956	8.9145	9.1520	9.1792	11.693	$71.071^{1.305}_{-1.331}$	$0.746^{0.018}_{-0.019}$
BAO 15	9.5942	9.0961	8.6801	8.5424	8.600	$66.179^{2.984}_{-3.092}$	$0.637^{0.066}_{-0.078}$

**Table 3.**  $\chi^2$  values of the reconstructions and best fit  $\Lambda$ CDM models.

	RBF		Mat72		Poly2		Poly3		$\Lambda$ CDM	
	$z_{t_1}$	$z_{t_2}$	$z_{t_1}$	$z_{t_2}$	$z_{t_1}$	$z_{t_2}$	$z_{t_1}$	$z_{t_2}$	$z_{t_1}$	$z_{t_2}$
Hz 57	0.6242	-	0.6218	-	0.7375	-	0.7467	-	0.7732	-
CC 32	0.5603	1.6050	0.5411	1.4382	0.6734	-	0.6868	-	0.6222	-
BAO 18	0.5577	-	0.5556	-	0.6905	-	0.7119	-	0.8106	-
BAO 15	-	-	-	-	0.5533	-	0.5335	-	0.5396	-

**Table 4.** Transition redshifts for the reconstructions and best fit  $\Lambda$ CDM models.

## Acknowledgments

HKJ thanks NCRA-TIFR, Pune for hospitality, as this manuscript was completed during a sabbatical from IISER Mohali.

## References

- [1] N. Aghanim, Y. Akrami, F. Arroja, M. Ashdown, J. Aumont, C. Baccigalupi et al., *Planck 2018 results-i. overview and the cosmological legacy of planck*, *Astronomy & Astrophysics* **641** (2020) A1.
- [2] DES collaboration, *Dark energy survey year 3 results: Cosmological constraints from galaxy clustering and weak lensing*, *Phys. Rev. D* **105** (2022) 023520 [2105.13549].

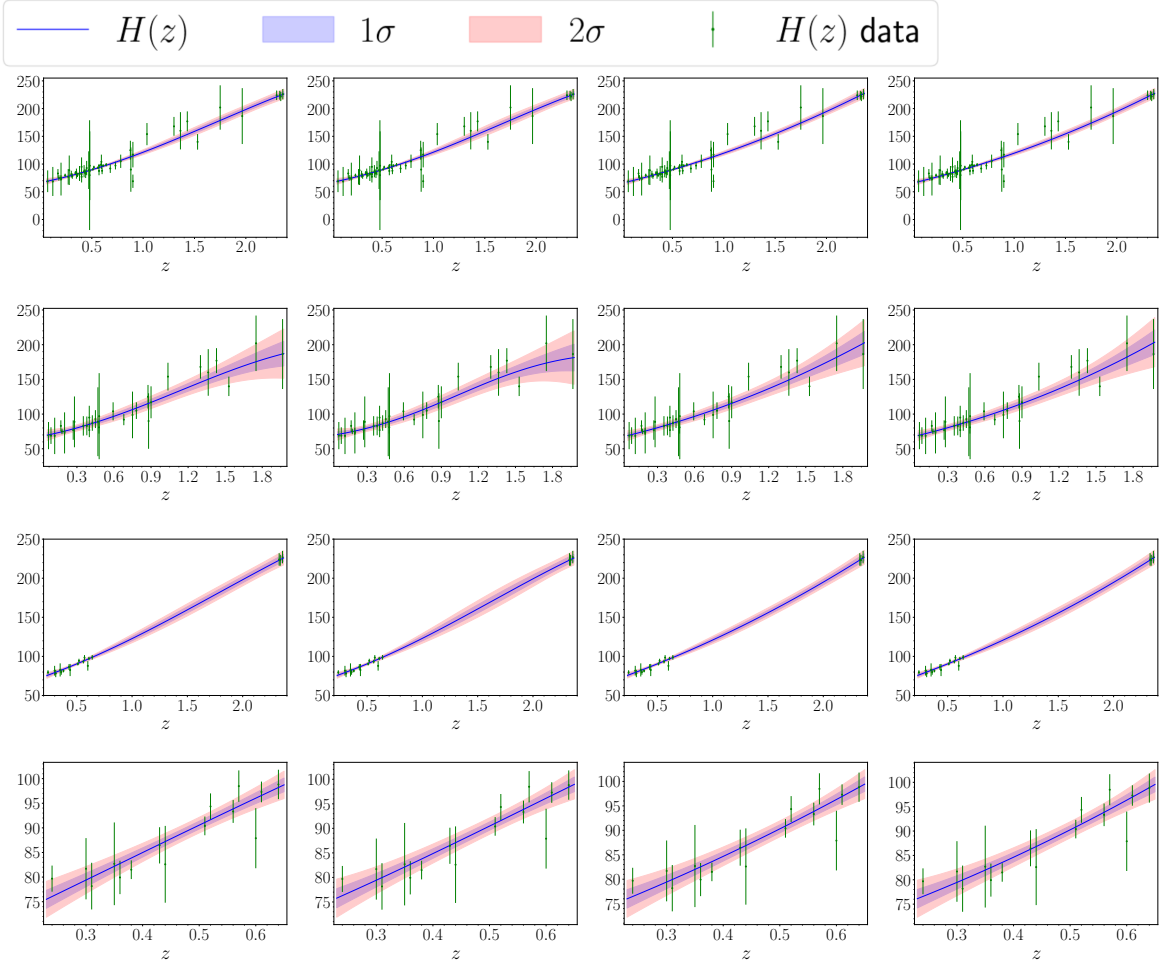


**Figure 4.** Evolution of the Hubble parameter. Top to bottom: Hz 57, CC 32, BAO18, BAO15. Left to right: RBF, Mat72, Poly2, Poly3

- [3] T. Abbott, M. Acevedo, M. Aguena, A. Alarcon, S. Allam, O. Alves et al., *The dark energy survey: Cosmology results with  $\sim 1500$  new high-redshift type ia supernovae using the full 5-year dataset*, *arXiv preprint arXiv:2401.02929* (2024) .
- [4] A.G. Riess, A.V. Filippenko, P. Challis, A. Clocchiatti, A. Diercks, P.M. Garnavich et al., *Observational evidence from supernovae for an accelerating universe and a cosmological constant*, *The astronomical journal* **116** (1998) 1009.
- [5] G. Hinshaw, D. Larson, E. Komatsu, D.N. Spergel, C. Bennett, J. Dunkley et al., *Nine-year wilkinson microwave anisotropy probe (wmap) observations: cosmological parameter results*, *The Astrophysical Journal Supplement Series* **208** (2013) 19.
- [6] N. Aghanim, Y. Akrami, M. Ashdown, J. Aumont, C. Baccigalupi, M. Ballardini et al., *Planck 2018 results-vi. cosmological parameters*, *Astronomy & Astrophysics* **641** (2020) A6.
- [7] S. Weinberg, *The cosmological constant problem*, *Reviews of modern physics* **61** (1989) 1.
- [8] S.M. Carroll, *The cosmological constant*, *Living reviews in relativity* **4** (2001) 1.
- [9] P.J.E. Peebles and B. Ratra, *The cosmological constant and dark energy*, *Reviews of modern physics* **75** (2003) 559.

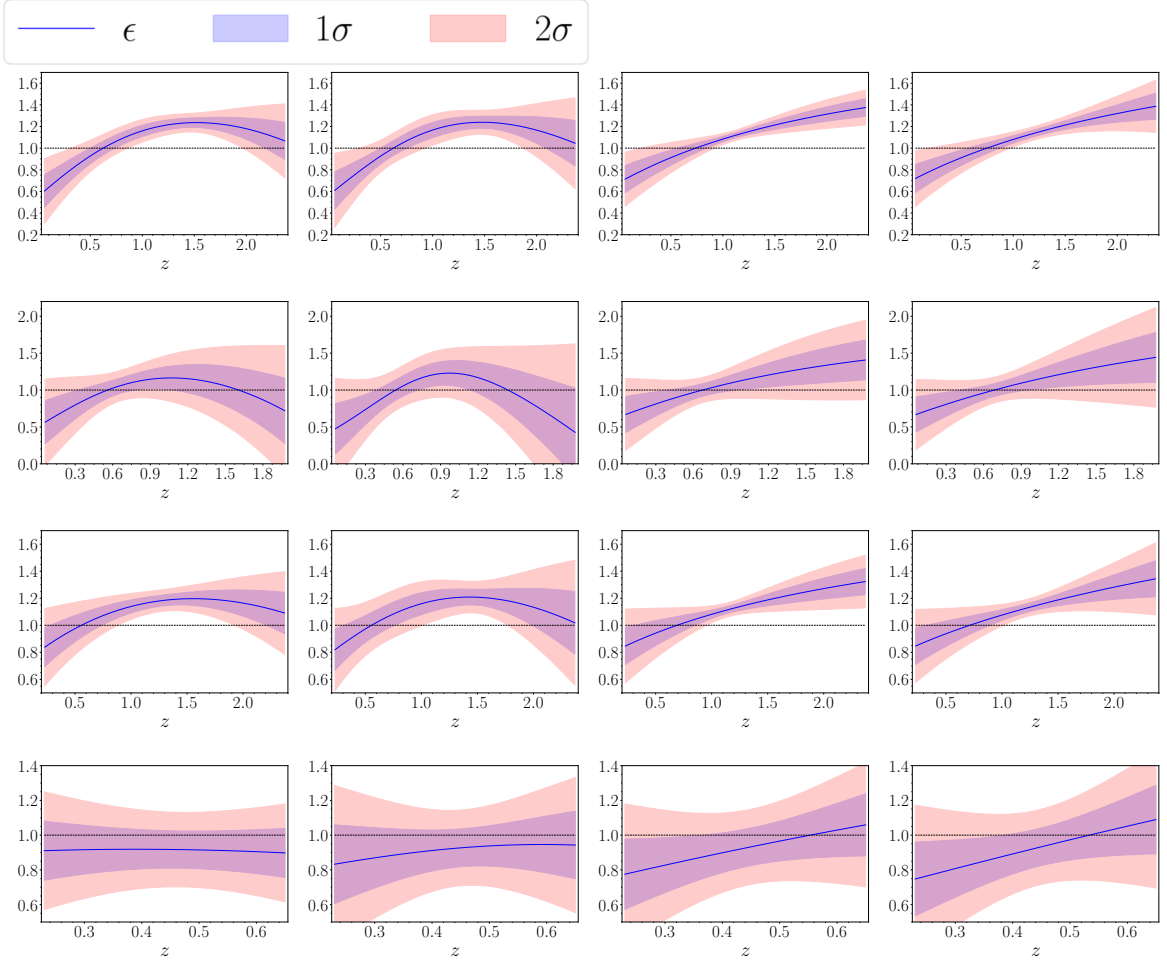


**Figure 5.** Evolution of the slow-roll parameter  $\epsilon$ . Top to bottom: Hz 57, CC 32, BAO18, BAO15. Left to right: RBF, Mat72, Poly2, Poly3

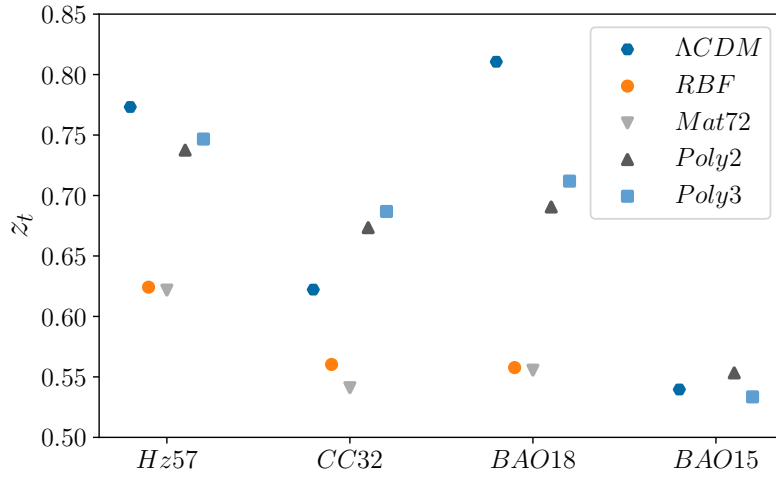


**Figure 6.**  $z_t$  values for the GP reconstructions and the best-fit  $\Lambda$ CDM model for the different datasets.

- [10] E.J. Copeland, M. Sami and S. Tsujikawa, *Dynamics of dark energy*, *International Journal of Modern Physics D* **15** (2006) 1753.
- [11] B. Ratra and P.J. Peebles, *Cosmological consequences of a rolling homogeneous scalar field*, *Physical Review D* **37** (1988) 3406.
- [12] M. Chevallier and D. Polarski, *Accelerating universes with scaling dark matter*, *International Journal of Modern Physics D* **10** (2001) 213.
- [13] A. Tripathi, A. Sangwan and H. Jassal, *Dark energy equation of state parameter and its evolution at low redshift*, *Journal of Cosmology and Astroparticle Physics* **2017** (2017) 012.
- [14] A. Sangwan, A. Tripathi and H. Jassal, *Observational constraints on quintessence models of dark energy*, *arXiv preprint arXiv:1804.09350* (2018) .
- [15] J.P. Johnson and S. Shankaranarayanan, *Cosmological perturbations in the interacting dark sector: Mapping fields and fluids*, *Phys. Rev. D* **103** (2021) 023510 [[2006.04618](#)].
- [16] M.P. Rajvanshi, A. Singh, H. Jassal and J. Bagla, *Tachyonic vs quintessence dark energy: linear perturbations and cmb data*, *Classical and Quantum Gravity* **38** (2021) 195001.
- [17] W.J. Wolf and P.G. Ferreira, *Underdetermination of dark energy*, *Physical Review D* **108** (2023) 103519 [[2310.07482](#)].
- [18] W.J. Wolf, C. García-García and P.G. Ferreira, *Robustness of dark energy phenomenology across different parameterizations*, [2502.04929](#).
- [19] T.P. Sotiriou and V. Faraoni,  *$f(R)$  theories of gravity*, *Reviews of Modern Physics* **82** (2010) 451.
- [20] A. De Felice and S. Tsujikawa,  *$f(R)$  theories*, *Living Reviews in Relativity* **13** (2010) 1.
- [21] W. Hu and I. Sawicki, *Models of  $f(R)$  Cosmic Acceleration that Evade Solar-System Tests*, *Physical Review D* **D76** (2007) 64004 [[0705.1158](#)].
- [22] J.P. Johnson and S. Shankaranarayanan, *Low-energy modified gravity signatures on the large-scale structures*, *Physical Review D* **100** (2019) 083526.
- [23] S. Shankaranarayanan and J.P. Johnson, *Modified theories of gravity: Why, how and what?*, *Gen. Rel. Grav.* **54** (2022) 44 [[2204.06533](#)].
- [24] L. Verde, T. Treu and A.G. Riess, *Tensions between the early and the late universe*, *Nature Astron.* **3** (2019) 891.
- [25] E. Di Valentino, O. Mena, S. Pan, L. Visinelli, W. Yang, A. Melchiorri et al., *In the realm of the hubble tension—a review of solutions*, *Class. Quant. Grav.* **38** (2021) 153001 [[2103.01183](#)].
- [26] D. Huterer and G. Starkman, *Parameterization of dark-energy properties: A principal-component approach*, *Phys. Rev. Lett.* **90** (2003) 031301 [[astro-ph/0207517](#)].
- [27] A. Shafieloo, U. Alam, V. Sahni and A.A.A. Starobinsky, *Smoothing supernova data to reconstruct the expansion history of the Universe and its age*, *Monthly Notices of the Royal Astronomical Society* **366** (2006) 1081 [[astro-ph/0505329](#)].
- [28] V. Sahni, T.D. Saini, A.A. Starobinsky and U. Alam, *Statefinder: A new geometrical diagnostic of dark energy*, *JETP Lett.* **77** (2003) 201 [[astro-ph/0201498](#)].
- [29] M. Visser, *Cosmography: Cosmology without the einstein equations*, *Gen. Rel. Grav.* **37** (2005) 1541 [[gr-qc/0411131](#)].
- [30] A. Shafieloo, A.G. Kim and E.V. Linder, *Gaussian process cosmography*, *Physical Review D* **85** (2012) 123530 [[1204.2272](#)].
- [31] A. Aviles, C. Gruber, O. Luongo and H. Quevedo, *Cosmography and constraints on the equation of state of the universe in various parametrizations*, *Phys. Rev. D* **86** (2012) 123516 [[1204.2007](#)].

- [32] V. Sahni and A. Starobinsky, *Reconstructing dark energy*, *Int. J. Mod. Phys. D* **15** (2006) 2105 [[astro-ph/0610026](#)].
- [33] C. Cattoen and M. Visser, *The hubble series: Convergence properties and redshift variables*, *Class. Quant. Grav.* **24** (2007) 5985 [[0710.1887](#)].
- [34] C. Clarkson and C. Zunckel, *Direct reconstruction of dark energy*, *Physical Review Letters* **104** (2010) 211301 [[1002.5004](#)].
- [35] Z. Li, J.E. Gonzalez, H. Yu, Z.-H. Zhu and J.S. Alcaniz, *Constructing a cosmological model-independent hubble diagram of type ia supernovae with cosmic chronometers*, *Physical Review D* **93** (2016) 043014 [[1504.03269](#)].
- [36] A. Aviles, J. Klapp and O. Luongo, *Toward unbiased estimations of the statefinder parameters*, *Phys. Dark Univ.* **17** (2017) 25 [[1606.09195](#)].
- [37] DESI collaboration, *Desi 2024: reconstructing dark energy using crossing statistics with desi dr1 bao data*, *Journal of Cosmology and Astroparticle Physics* **10** (2024) 048 [[2405.04216](#)].
- [38] J.L. Bernal, L. Verde and A.G. Riess, *The trouble with  $h_0$* , *Journal of Cosmology and Astroparticle Physics* **10** (2016) 019 [[1607.05617](#)].
- [39] D.K. Hazra, B. Beringue, J. Errard, A. Shafieloo and G.F. Smoot, *Exploring the discrepancy between planck pr3 and act dr4*, *Journal of Cosmology and Astroparticle Physics* **12** (2024) 038 [[2406.06296](#)].
- [40] T.L. Smith, M. Lucca, V. Poulin, G.F. Abellan, L. Balkenhol, K. Benabed et al., *Hints of early dark energy in planck, spt, and act data: New physics or systematics?*, *Physical Review D* **106** (2022) 043526 [[2202.09379](#)].
- [41] E.J. Copeland, A.R. Liddle and D. Wands, *Exponential potentials and cosmological scaling solutions*, *Physical Review D* **57** (1998) 4686.
- [42] T. Barreiro, E.J. Copeland and N.a. Nunes, *Quintessence arising from exponential potentials*, *Physical Review D* **61** (2000) 127301.
- [43] A. Sangwan, A. Mukherjee and H. Jassal, *Reconstructing the dark energy potential*, *Journal of Cosmology and Astroparticle Physics* **2018** (2018) 018.
- [44] M.P. Rajvanshi and J. Bagla, *Reconstruction of dynamical dark energy potentials: Quintessence, tachyon and interacting models*, *Journal of Astrophysics and Astronomy* **40** (2019) 1.
- [45] B. L’Huillier, A. Shafieloo, E.V. Linder and A.G. Kim, *Model independent expansion history from supernovae: Cosmology versus systematics*, *Monthly Notices of the Royal Astronomical Society* **485** (2019) 2783 [[1812.03623](#)].
- [46] C. Dvorkin et al., *Machine learning and cosmology*, in *Snowmass 2021*, 3, 2022 [[2203.08056](#)].
- [47] T. Lu, Z. Haiman and J.M.Z. Matilla, *Simultaneously constraining cosmology and baryonic physics via deep learning from weak lensing*, *Mon. Not. Roy. Astron. Soc.* **511** (2022) 1518 [[2109.11060](#)].
- [48] K. Dialektopoulos, J.L. Said, J. Mifsud, J. Sultana and K.Z. Adami, *Neural network reconstruction of late-time cosmology and null tests*, *Journal of Cosmology and Astroparticle Physics* **02** (2022) 023 [[2111.11462](#)].
- [49] R. Sharma, A. Mukherjee and H.K. Jassal, *Reconstruction of latetime cosmology using principal component analysis*, *European Physica Journal Plus* **137** (2022) 219 [[2004.01393](#)].
- [50] P. Mukherjee, J. Levi Said and J. Mifsud, *Neural network reconstruction of  $h'(z)$  and its application in teleparallel gravity*, *Journal of Cosmology and Astroparticle Physics* **12** (2022) 029 [[2209.01113](#)].

- [51] K.F. Dialektopoulos, P. Mukherjee, J. Levi Said and J. Mifsud, *Neural network reconstruction of cosmology using the pantheon compilation*, *European Physics Journal C* **83** (2023) 956 [2305.15499].
- [52] C. Bengaly, M.A. Dantas, L. Casarini and J. Alcaniz, *Measuring the hubble constant with cosmic chronometers: a machine learning approach*, *European Physics Journal C* **83** (2023) 548 [2209.09017].
- [53] R. Sharma and H.K. Jassal, *Inference of cosmological models with principal component analysis*, *J. Astrophys. Astron.* **45** (2024) 24 [2211.13608].
- [54] E.E.O. Ishida and R.S. de Souza, *Hubble parameter reconstruction from a principal component analysis: minimizing the bias*, *Astron. Astrophys.* **527** (2011) A49 [1012.5335].
- [55] R.A. Banerjee, S., *Linear Algebra and Matrix Analysis for Statistics*, Chapman and Hall/CRC (2014), 10.1201/b17040.
- [56] M. Seikel, C. Clarkson and M. Smith, *Reconstruction of dark energy and expansion dynamics using Gaussian processes*, *Journal of Cosmology and Astroparticle Physics* **2012** (2012) 036 [1204.2832].
- [57] T. Yang, Z.-K. Guo and R.-G. Cai, *Reconstructing the interaction between dark energy and dark matter using gaussian processes*, *Physical Review D* **91** (2015) 123533 [1505.04443].
- [58] H. Zhang, Y. Liu, H. Yu, X. Nong, N. Liang and P. Wu, *Constraints on cosmological models from quasars calibrated with type Ia supernova by a Gaussian process*, *Monthly Notices of the Royal Astronomical Society* **530** (2024) 4493 [2404.15913].
- [59] T. Beckers, *An introduction to gaussian process models*, 2102.05497.
- [60] J.d.J. Velázquez, L.A. Escamilla, P. Mukherjee and J.A. Vázquez, *Non-parametric reconstruction of cosmological observables using Gaussian Processes Regression*, 2410.02061.
- [61] C.E. Rasmussen and C.K.I. Williams, *Gaussian Processes for Machine Learning*, The MIT Press (2006).
- [62] C.M. Bishop, *Pattern Recognition and Machine Learning (Information Science and Statistics)*, Springer-Verlag, Berlin, Heidelberg (2006).
- [63] A. Bouali, H. Chaudhary, R. Hama, T. Harko, S.V. Sabau and M.S. Martín, *Cosmological tests of the osculating Bartheł–Kropina dark energy model*, *European Physical Journal C* **83** (2023) 121 [2301.10278].
- [64] B. Xu, J. Xu, K. Zhang, X. Fu and Q. Huang, *Model-independent test of the running Hubble constant from the Type Ia supernovae and the Hubble parameter data*, *Monthly Notices of the Royal Astronomical Society* **530** (2024) 5091.
- [65] H. Yu, B. Ratra and F.-Y. Wang, *Hubble Parameter and Baryon Acoustic Oscillation Measurement Constraints on the Hubble Constant, the Deviation from the Spatially Flat  $\Lambda$ CDM Model, the Deceleration–Acceleration Transition Redshift, and Spatial Curvature*, *Astrophys. J.* **856** (2018) 3 [1711.03437].